Version of Record: https://www.sciencedirect.com/science/article/pii/S037877882200682X
Manuscript_71d2b5bd7e6642c6e7d402ca0efc5e99

Enhancement of phase change material hysteresis model: a case study of modeling building envelope in EnergyPlus

Fan Feng, Yangyang Fu, Zhiyao Yang, Zheng O'Neill*

J. Mike Walker '66 Department of Mechanical Engineering,

Texas A&M University, College Station, TX, 77843, United States

*Corresponding Author: zoneill@tamu.edu

ABSTRACT

Nowadays, buildings are expected to offer demand side services to the power grid to enhance the electrical load flexibility, which leads to the concepts of grid-interactive efficient buildings (GEBs). Phase change material (PCM)-based thermal energy storage has seen increasing attention in recent years for peak load shifting of grid-interactive efficient buildings (GEBs). Numerical models are critical tools for design and evaluation of PCM-integrated systems. Most industrial-grade PCMs are reported to melt/freeze over a temperature range instead of at a unique temperature. Such thermal hysteresis effect significantly affects the reliability of simulation results because not only the heat transfer process depends on melting and freezing temperatures, the PCM thermal properties change significantly during the phase change process as well. This study is aimed to develop a model for the PCMs used in the building envelope with the capability to accurately simulate hysteretic behaviors. This model is based on a two-phase assumption and is implemented in a whole building energy performance simulation program (i.e., EnergyPlus). A comparison between numerical results and experimental data shows that during a complete phase transition, the proposed method could achieve a good agreement with the experimental data. During a partial phase transition, the proposed method could lead to significant improvements compared to other alternative PCM models, including the existing PCM model in EnergyPlus. Last, whole building simulations were performed to study this model's performance regarding heating/cooling loads and zone mean air temperature of a given building. The results show that the difference in hourly heating/cooling loads introduced by the models was less than 1% in design conditions, while significant changes were observed in both hourly heating/cooling loads and zone mean air temperature when the PCM envelope underwent partial phase transition processes.

Keywords: building simulation; Phase change materials (PCM); EnergyPlus; PCM hysteresis

Nomenclature	
c_p	specific heat capacity, J/kg·K
h	enthalpy, J/g
k	thermal conductivity, W/m·K

LH	latent heat, kJ/kg
m	mass, kg
ρ	density, kg/m^3
r	mass ratio
t	time step
τ	parameter of the $\xi - T$ function
T	temperature, K
Δx	space interval, m
Δt	time interval, s
ξ	phase fraction

Acronyms

BPS	Building Performance Simulation
DSC	Differential Scanning Calorimetry
HVAC	Heating, ventilation, and air conditioning
MBE	Mean bias error
PCM	Phase Change Material
RMSE	Root mean square error
SSE	Sum of the squared error

Subscripts

α	part α of the phase change material
β	part β of the phase change material
γ	the phase change material itself
err	error
freezing	freezing process
i	i^{th} surface node
j	j^{th} timestep
liq	liquid state
melting	melting process
p	peak temperature
solid	solid state

1. Introduction

The use of phase change materials (PCMs) in buildings has seen a significant increase in research, development, and implementation during the past decade. Solid/liquid PCMs that store heat or cold in melting and freezing processes are most used in buildings for various scenarios, including building envelopes (wall, glazing, roof, etc.) [1-4] and HVAC components (e.g., thermal energy storage tank) [5-7]. In these scenarios, PCMs are considered as a beneficial solution because their high thermal energy storage capacity can reduce and delay the daily peak loads, leading to increased thermal comfort, energy savings, and HVAC system downsizing. For example, in the study [7], a heat pump coupled with a thermal energy storage tank was experimentally tested under simulated summer conditions. This system was then applied for space cooling to evaluate the cold storage behavior of the PCM tank. The results showed that the PCM tank was able to maintain the indoor air temperature 20.65% longer than a baseline case with a water tank and could shave the peak load effectively.

Studies evaluating the performance of PCM systems can be categorized as experimental and numerical. While experimental evaluations such as [8] could capture the actual operational characteristic of PCM-enhanced systems, their applications are limited due to the time and cost of experiment deployment and measurements. Numerical simulation, such as [9], on the other hand, provides a more cost-effective and time-efficient approach and has become more prevalent during the past few decades.

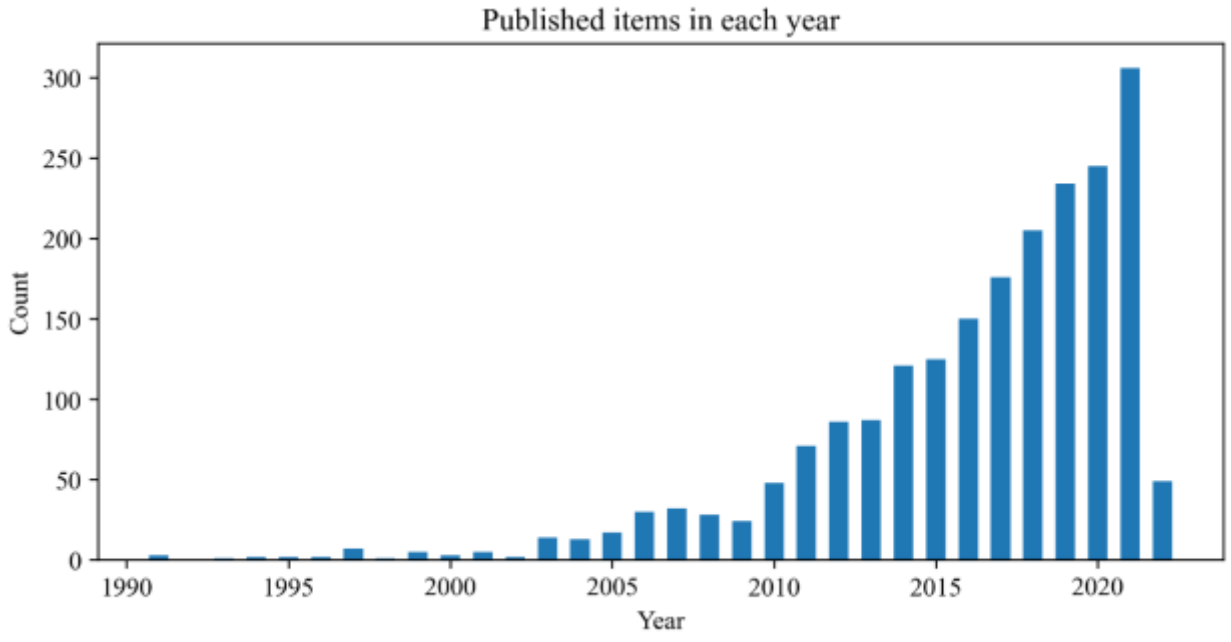

Figure 1. Number of indexed articles listed in the Web of Science database

Simulation investigations of PCM-enhanced systems require high-fidelity models of the PCM to accurately describe the phase change and transfer phenomenon. Figure 1 reports the annual number of published articles since 1990 retrieved from the Web of Science using "Phase Change Materials", "Simulation", and "Building" as keywords. The figure shows that the number of published studies on numerical simulation of PCMs in buildings has been increasing quickly since the 2010s.

For ideal and nearly ideal PCMs, the phase change phenomenon can be assumed to occur at a single temperature. However, the melting and freezing processes of industrial-grade PCMs, such as the one shown in Figure 2, take place over a temperature range [10]. In addition to hysteresis, sub-cooling in the freezing process – that is, freezing starts below the freezing point – further increases the non-ideal behavior. The importance of hysteresis and sub-cooling effects has been investigated and confirmed in [11, 12]. These non-ideal behaviors raise great challenges in developing simulation models of PCMs.

There have been many research works and papers on the modeling methods for the phase change processes in the past several decades. These models can be mainly categorized into two groups. One group of modeling methods addresses the phase change processes when PCMs undergo a complete phase change, which means phase changes consist of complete phase transitions from solid to liquid or vice versa. This set of models mainly focuses on the mathematical representations and determination of the two *h*-*T* curves, as shown in Figure 2. These models are relatively easy and do not represent any challenging problem. For example, in [13], Dolado et al. used polynomial functions to build the empirical models for these two *h*-*T* curves based on experimental data. The results showed that these polynomial models could achieve a relatively good agreement with the experimental data. Many other transition functions are also used to describe the *h*-*T* relationships, including the piecewise linear function in [14], the exponential function in [14], etc.

The other group of research works mainly addresses the computational models when partial phase changes are undertaken. That is, the phase transition from one state to another is interrupted before it is completed. Compared to complete phase change, it is more challenging to describe the behaviors of PCMs after interruptions. For example, the model proposed by Delcroix et al. [15] can achieve a good agreement with experimental data for a complete phase change process with hysteresis, but for a partial phase change process, a significant mismatch was observed between simulation results and experimental data. There are also a few other research papers attempting to address this issue, including the approaches proposed by Barz and Sommer [10], Bony and Citherlet [16], Goia et al. [17], etc. A detailed review of these approaches of phase change hysteresis will be presented in Section 2.1.

Based on the approach by Bony and Citherlet [16], Chandrasekharan et al. [18] presented an enhanced simulation module of PCMs in EnergyPlus, and this is also the current PCM hysteresis

model in EnergyPlus at the time of writing. This approach assumes that after the melting/freezing process is interrupted, the PCM will switch to the other curve and the transition process is modeled as a straight line between these two curves. However, based on experimental tests conducted by Delcroix et al. [15], after interruption a PCM would adopt an intermediate curve in the transition area between these two curves instead of directly switching to the other curve. This can also be confirmed in our case study section that a significant discrepancy between experimental data and the modeling result of the current EnergyPlus hysteresis method can be observed.

Therefore, a hysteresis method that better handles the hysteresis behavior is proposed in this study, which assumes that the PCM structure can be viewed as a mixture of solid and liquid materials, and a parameter—phase fraction is used to determine the PCM state during phase change processes. This hysteresis model will be referred to as the two-phase approach in this paper. This method is adapted from the static hysteresis model presented by Ivshin and Pence [19]. Another novelty of this work is implementing this two-phase hysteresis model in EnergyPlus to enhance the simulation capability for the PCM-based building components in whole building simulation program. There are also many other building performance simulation (BPS) programs that allow us to evaluate the PCM-based building components, such as TRNSYS [15, 20], Modelica [21], ESP-r[22], etc. With the proposed two-phase hysteresis method, the hysteresis simulation modules in these BPS programs can also be further enhanced.

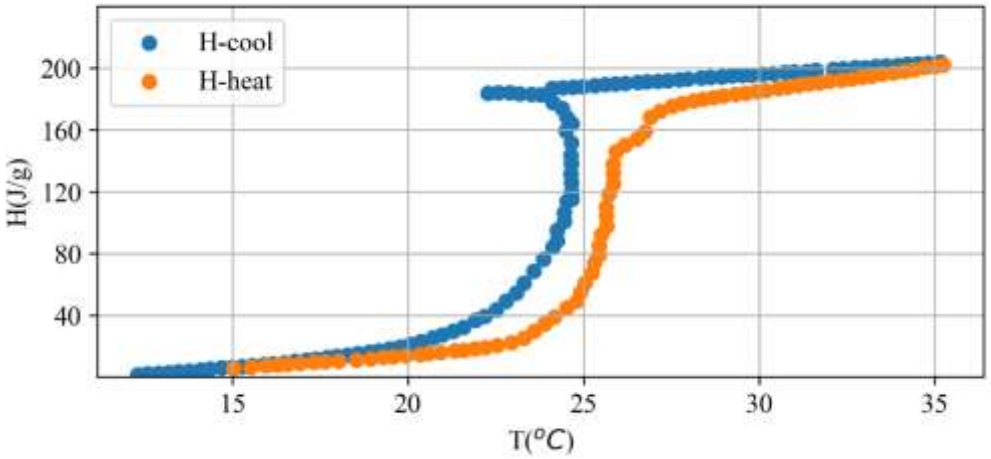

Figure 2. Enthalpy (H)-Temperature (T) performance curves of an industrial-grade PCM (RUBITHERM SP 26E [23])

The aims of the study in this paper are:

- To propose and develop a PCM model that can simulate the hysteresis effect of PCM-based building components, especially in partial phase change processes; and
- To analyze the effect of PCM model on building energy consumption estimation, system sizing, etc.; and

- To provide the community of researchers a PCM modeling tool that can be used to simulate the PCMs' load shifting capability and to design operating schemes that can better overcome the supply-demand gap.

This paper is structured as follows. First, a model is developed based on a two-phase assumption in [24] and then implemented for PCM-based building envelopes in a whole building simulation program, EnergyPlus [25]. The proposed model is validated with experimental data from [8] and compared with several other PCM models. Based on the model, a sensitivity analysis is then conducted on the impact of PCM property parameter uncertainty on the simulation accuracy to identify those to be measured with great care. Finally, the proposed two-phase method is used in whole-building simulations and compared with other existing PCM methods to demonstrate its enhanced accuracy.

2. Methodology

This section starts with a brief overview of existing studies on the PCM modeling method for building energy simulations, followed by a mathematical explanation of the proposed model and its implementation in EnergyPlus.

2.1. Overview of PCM models in building energy simulation

In this study, EnergyPlus is selected as the BPS tool to implement the proposed PCM hysteresis model. EnergyPlus is a whole building simulation program that integrates envelope, HVAC, water, and renewable energy source simulations and has now become a leading BPS tool after 20 years of updates [25]. EnergyPlus has a rich inventory of features for various simulation situations, including its heat balance-based solution for building thermal load, easy-to-use interfaces to other popular simulation programs and environments, the well-designed structure that facilitates adding new features, etc. Besides, it is free and open-source and has thus been widely used in many research and professional studies.

1). Heat transfer model of PCM in EnergyPlus

In BPS the heat transfer in building envelopes is usually simplified as one-dimensional process. These heat transfer problems are solved with two methods: the Conduction Transfer Function (CTF) method and the Conduction Finite Different method (CFD). The CTF method uses a single linear time series equation to describe the heat transfer process. Due to its simplicity and linearity, it can calculate the building load and surface temperatures in a time-efficient way and has been widely used in EnergyPlus and many other BPS programs. However, the CTF assumes constant material properties across the entire material and, therefore, cannot handle the dynamic thermal behavior of phase changing phenomenon. In contrast, the CFD method takes the property variation into account. In 2007, an implicit finite difference algorithm was developed and included in EnergyPlus to serve this purpose [25]. Figure 3 shows the grip points for a one-dimensional wall using the finite difference method. Based on this CFD algorithm, for an

internal node, the heat conduction transfer process could be solved by Eq. (1). This formulation allows the material properties such as density (ρ), thermal conductivity (k), and specific heat capacity (c_p) to be either constant or time-dependent.

$$\frac{\rho c_p \Delta x (T_{i,j} - T_{i,j-1})}{\Delta t} = \frac{k(T_{i-1,j} - T_{i,j})}{\Delta x} + \frac{k(T_{i+1,j} - T_{i,j})}{\Delta x} \quad (1)$$

where ρ is density, c_p is specific heat capacity, T indicates node temperature, k is thermal conductivity, Δx is position difference, and Δt is the time difference. Subscripts *i-1*, *i*, and *i+1* refer to nodes, and Subscripts *j* and *j-1* refer to appropriate time steps.

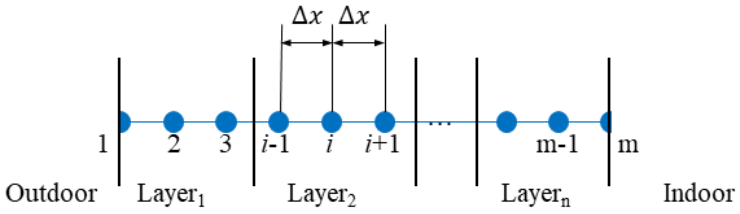

Figure 3. Grid points location for finite difference methods

Then, a second equation that calculates the material specific heat capacity c_p is required to account for the dynamic thermal behavior of PCMs, as shown in Eq. (2).

$$c_p = \frac{h_{i,j} - h_{i,j-1}}{T_{i,j} - T_{i,j-1}} \quad (2)$$

where *h* refers to enthalpy, and subscripts indicate nodes and appropriate time steps.

Besides, additional equations that relate enthalpy *h* and temperature *T* are used to describe the phase change behavior of PCMs, as shown in Eq. (3). In Pedersen's finite difference method in 2007 [26], the enthalpy-temperature curve is a single curve that describes both melting and freezing processes as shown in Figure *4*.

$$h_{i,j} = f(T_{i,j}) \quad (3)$$

where *f* is an enthalpy-temperature function that uses temperature to calculate the enthalpy value.

This model was then validated in the study by Tabares-Velasco et al. [27], which showed acceptable annual and monthly simulation accuracy was achieved for ideal/pure PCMs with a small time interval. The accuracy was assessed by Root Mean Square Error (RMSE) between EnergyPlus's PCM models and baseline models that use CTF without PCM in their study. To achieve accurate hourly simulation, a small node space was also required. However, significant accuracy issues were identified for PCMs with strong hysteresis behaviors, as shown in Figure *4*.

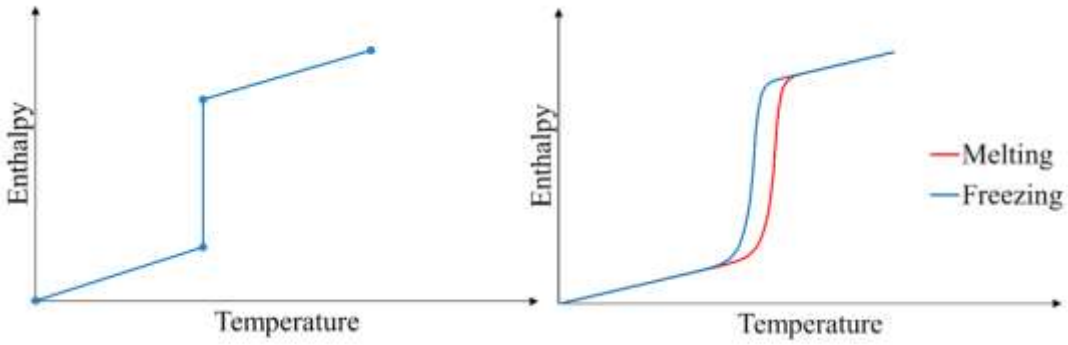

(a) (b)

Figure 4. Enthalpy-temperature curves for (a) ideal/pure PCMs and (b) industrial-grade PCMs with hysteresis behaviors

2). Hysteresis behaviors

Hysteresis of PCMs is defined as the discrepancy between the melting and freezing process, as shown in Figure 4(b). Hysteresis is mainly due to primary nucleation and crystal growth mechanisms, which lower the crystallizing temperature compared to the melting temperature [28]. As a result, two separate functions are needed to represent the enthalpy-temperature relationships during melting and freezing, respectively. In addition, special attention is required to the transition region and transitional behavior between the melting and freezing curves when PCMs are undergoing partial phase change processes.

3). Current modeling approaches for transitional behaviors

There are already several studies of the incomplete phase change process in transition regions. The first method, usually called the "one-curve method" [18], assumes that a PCM will follow the same curve when the phase change process is interrupted. For example, if the temperature of a material, which is initially increased on the melting curve in the transition region, is decreased suddenly(see point 1 in Figure 5(a)), the phase change process will follow the melting curve in the reverse direction until the next interruption occurs (see point 2a in Figure 5(a)). This means that the hysteresis behavior for such materials could only be observed when it is cooled from a complete liquid state. The transition from freezing to melting is similar, as illustrated in Figure 5(b).

Bony and Citherlet [16] proposed a different approach in that the transition between melting and freezing curves is a straight line. For example, if the melting process is interrupted (see point 1 in Figure 5(a)), the PCM will follow a straight line 1-n between the freezing curve and the melting curve to reach the freezing curve. This cooling process will continue until the next interruption (see point 2c). Also, the transition from freezing to melting can be observed in Figure 5(b). More detail about the mathematical representation of the switching lines is provided in [18].

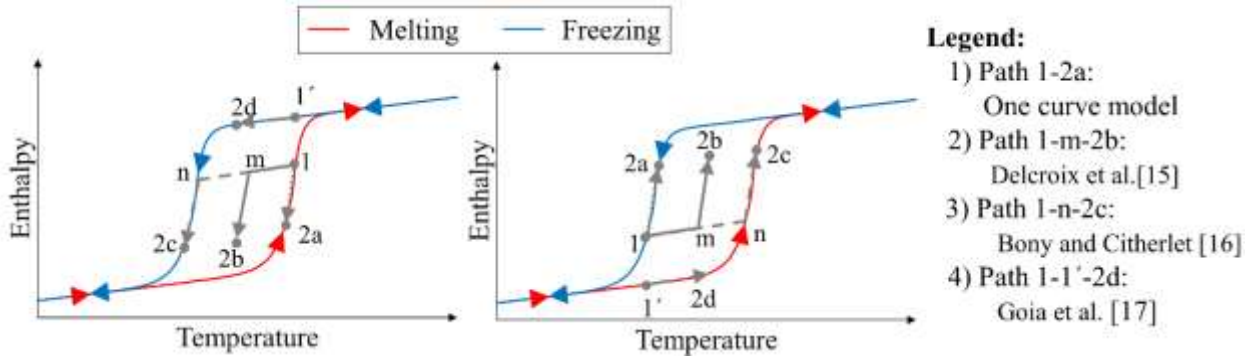

Figure 5. Transitional model: (a) interrupted heating scenario (b) interrupted cooling scenario

Besides, Goia et al. [17] proposed that the PCM will follow the process indicated by path 1-1´-2d in Figure 5 if a phase change process is interrupted. In their study, if an interruption is observed, the PCM will directly assume another phase change curve.

Recently, experimental tests conducted by Delcroix et al. [15] showed that instead of the aforementioned three paths, an organic PCM would adopt an intermediate curve between the melting and freezing curves and proceed to point 2b as indicated by path 1-m-2b. This outcome suggests that it is necessary to develop another modeling method that could account for such intermediate behavior.

2.2. The two-phase modeling approach

1). The two-phase assumption

The proposed two-phase modeling approach assumes that PCMs could be viewed as a mixture of solid and liquid materials over the temperature range. This approach has already been successfully applied to PCMs in a study [29]. According to this approach, PCMs could be quantified by a characteristic parameter–phase fraction, which is defined as the ratio of the mass of liquid materials to the mass of both solid and liquid materials, as shown in Eq. (4).

$$\xi = \frac{m_{liq}}{m_{liq}+m_{solid}}, \tag{4}$$

where ξ denotes the phase fraction, and m_{liq} and m_{solid} are the masses of solid and liquid phases, respectively. This parameter ξ could take a value between 0 (fully solid) and 1 (fully liquid) to represent the PCM state. In the following subsections, a hysteresis transitional model is developed based on this assumption.

2). The proposed hysteresis transitional model

Based on the aforementioned two-phase assumption, a PCM is considered as two distinct parts, and each part follows different curves. Taking an interrupted melting as an example, as shown in Figure 6(a), the PCM is initially melting along the melting curve in the transitional region, and at timestep t_j, its temperature is decreased (see point $\gamma(t_j)$). According to the two-phase assumption,

the PCM, denoted as γ, could be viewed as a mixture of two parts--α and β and the phase fractions of these two parts at timestep t_j are $\xi_\alpha(t_j)$ and $\xi_\beta(t_j)$, respectively. In this case, part β is completely solid (see point $\beta(t_j)$), which means $\xi_\beta(t_j)$ is zero, and its mass ratio of the total PCM is assumed to be r_β. Part α is located on the freezing curve (see point $\alpha(t_j)$), and its mass ratio is r_α. Therefore, the relationship between $\xi_\alpha(t_j)$, $\xi_\beta(t_j)$ and $\xi_\gamma(t_j)$ could be determined by Eq. (5).

$$\xi_\alpha(t_j) \cdot r_\alpha(t_j) + \xi_\beta(t_j) \cdot r_\beta(t_j) = \xi_\gamma(t_j) \tag{5a}$$

$$r_\alpha + r_\beta = 1 \tag{5b}$$

where r_α and r_β are the mass ratios of part α and part β to the total PCM γ, and could be mathematically expressed as $r_\alpha = \frac{m_\alpha}{m_\gamma}$ and $r_\beta = \frac{m_\beta}{m_\gamma}$.

In addition, two-phase fraction-temperature ($\xi - T$) curves for both freezing and melting processes will be constructed to calculate the phase fraction value based on the current temperature. The construction of these two $\xi - T$ curves will be discussed later in the following section. As shown in Figure 6(a), point α is on the freezing curve, and its phase fraction could be determined by current temperature T_j, where $\xi_\alpha(t_j)$ equals to $\xi_{\text{freezing}}(T_j)$. Point β is in a completely solid state, and its phase fraction is zero. Then, at the timestep t_j, Eq. (5a) could be converted to the following equation.

$$\xi_{freezing}(T_j) \cdot r_\alpha + 0 \cdot r_\beta = \xi_\gamma(t_j) \tag{6}$$

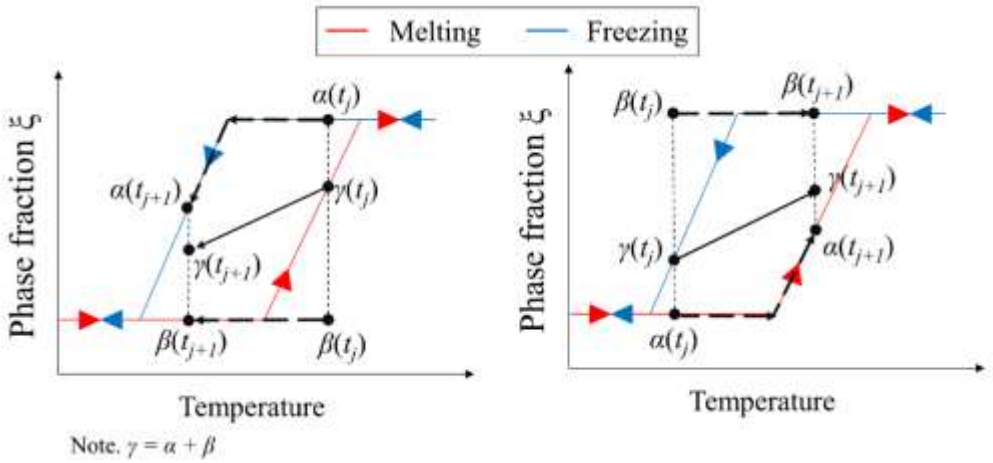

(a) (b)

Figure 6. Two-phase hysteresis model (a) interrupted melting scenario (b) interrupted freezing scenario

In addition, all the state variables of the PCM at the timestep t_j, including the current phase fraction $\xi_\gamma(t_j)$, current temperature T_j, etc. are known when we are calculating the state of the

PCM at the timestep t_{j+1}. By solving Eq. (6) and Eq. (5b), the mass ratio values r_α and r_β could be uniquely determined.

Then, these two parts α and β will proceed separately until the next timestep t_{j+1} (see points $a(t_{j+1})$ and $\beta(t_{j+1})$ in Figure 6), and the PCM temperature becomes T_{j+1}. The phase fractions of both part α and β at timestep t_{j+1} become $\xi_\alpha(t_{j+1})$ and $\xi_\beta(t_{j+1})$, respectively, and could then be computed based on the two-phase fraction-temperature ($\xi - T$) curves. That is, $\xi_\alpha(t_{j+1})$ is $\xi_{freezing}(T_{j+1})$ and $\xi_\beta(t_{j+1})$ is still zero because part β is in a solid phase. With the mass ratios of part α and part β, the total phase fraction at timestep t_{j+1} , $\xi_\gamma(t_{j+1})$, could be obtained by weighted summing the phase fractions of part α and part β. These behaviors for the cooling case are illustrated by the hysteresis algorithm represented by Eq. (7a). Similarly, the hysteresis algorithm for the heating case could also be derived, as shown in Eq. (7b).

$$\xi_\gamma(t_{j+1}) = \xi_{freezing}(T_{j+1}) \cdot \frac{\xi_\gamma(t_j)}{\xi_{freezing}(T_j)} \qquad \text{if } T_{j+1} \leq T_1 \tag{7a}$$

$$\xi_\gamma(t_{j+1}) = 1 - \frac{1-\xi_\gamma(t_j)}{1-\xi_{melting}(T_j)} \cdot (1 - \xi_{melting}(T_{j+1})) \qquad \text{if } T_{j+1} > T_j \tag{7b}$$

However, we still need an approach that yields the specific heat capacity and enthalpy of the PCM based on the phase fraction. The approach employed in this study is taken from Gaur and Wunderlich [29]. According to Gaur and Wunderlich [29], the specific heat capacity of the PCM in a transition region is approximately a linear combination of the contributions from sensible heat and the contributions from latent heat, as shown in Eq. (8).

$$c_{p,\xi} := \xi c_{p,liq} + (1-\xi) c_{p,solid} + \frac{d\xi}{dT} h_{latent} \tag{8}$$

where $c_{p,liq}$ and $c_{p,solid}$ are liquid-state and solid-state specific heat capacities, respectively, and h_{latent} is the latent heat released or absorbed during the phase change process. All these three values are property parameters of the PCMs, which are usually available from experiments or manufacturers' data sheets. It should be noted the latent terms could be approximated by a discrete form as shown in Eq. (9).

$$c_{p,\xi} := \xi c_{p,liq} + (1-\xi) c_{p,solid} + \frac{\Delta\xi}{\Delta T} h_{latent} \tag{9}$$

With specific heat capacity, the enthalpy of the PCM could be easily updated with Eq. (10).

$$h_{j+1} = h_j + c_{p,\xi} \cdot (T_{j+1} - T_j) \tag{10}$$

3) Construction of phase fraction-temperature ($\xi - T$) curve

In the current version of EnergyPlus (i.e., EnergyPlus 9.6 [30] used for this study), three-parameter exponential functions, taken from a study by Egolf and Manz [14], are used to describe the enthalpy-temperature (*H*-*T*) curves. Therefore, in our approach, a similar three-parameter exponential function is also used to represent the phase fraction-temperature ($\xi - T$) curves. The reasons are two-fold. First, the existing studies suggest that three-parameter exponential functions could achieve a good agreement between experimental and modeling, as presented in [18]. Second, when implementing the proposed hysteresis model in EnergyPlus, we could directly utilize the current input interface if our model inputs are consistent with current EnergyPlus PCM hysteresis model inputs.

The $\xi - T$ functions employed in our model are shown in Eq. (11) and Eq. (12), where T_p, τ_1, and τ_2 are model parameters and should be fitted from the measurement data. These data are usually available from both experiments (e.g., Differential Scanning Calorimetry DSC measurements) or manufacturers' data sheets. The curve fitting process will be illustrated in later sections.

$$\xi(T) = \frac{1}{2}\left(e^{\frac{-2|T-T_p|}{\tau_1}}\right) \qquad \text{for } T \leq T_p \tag{11}$$

$$\xi(T) = 1 - \frac{1}{2}\left(e^{\frac{-2|T-T_p|}{\tau_2}}\right) \qquad \text{for } T > T_p \tag{12}$$

It should be noted that there are also many other different functions for the $\xi - T$ curves, including piecewise linear functions, polynomial functions, or the Weibull density function used in [24]. Further details could be obtained in [31, 32], and based on their study, the three-parameter functions employed in this study could achieve comparable estimation accuracy without requiring too many parameters.

2.3. Implementation in EnergyPlus

The proposed hysteresis transitional model was then coded to the EnergyPlus program to replace the current phase transition calculation method. The implementations of the existing hysteresis model consist of two parts. The first part implements the conduction finite-difference solution algorithms, which were first added to EnergyPlus in version 2.0, released in April 2007 [33]. This algorithm uses a semi-implicit finite difference method with auxiliary enthalpy-temperature functions to account for the phase transition process. The enthalpy-temperature functions are implemented in the second part, where a phase transitional model is also implemented. Therefore, the proposed hysteresis transitional model could be implemented by mainly modifying two source code files associated with these two parts. Most modifications were replacing existing phase transition process methods with the proposed method. All source codes and executable file for this modified EnergyPlus version has been uploaded to the Github repository [34].

3. Model Validation

The proposed PCM model is tested against the experimental data from Goia et al. [8, 17] taken on a commercially available PCM product from Rubitherm [23]. The proposed PCM hysteresis model is also compared with the existing PCM hysteresis model in EnergyPlus. In this section, the procedure to construct $\xi - T$ curves from the property data of the PCM product is discussed, followed by a brief introduction to the experimental setup in [8, 17]. Then the comparison of the results is presented and discussed. Finally, a whole building simulation case study of a PCM-based building envelope is presented to show the impact of different hysteresis models on the building energy performance and sizing results of the HVAC system.

3.1. Construction of $\xi - T$ curve functions from measurements

Differential Scanning Calorimetry (DSC) is a widely used method to measure thermal behavior. The plot (a) in Figure 7 shows the original recorded DSC signals for both heating and cooling processes. It could be observed that there is a clear hysteresis behavior as the melting and freezing peak curves reach their peaks at different temperatures. Cumulative DSC curves, as shown in plot (b), could be generated by integrating the original recorded DSC signals over the temperature. These two curves are also the enthalpy-temperature curves of the material. The sensible heat capacity is then calculated from the property data in Table 1 and subtracted from the cumulative DSC signals. The results from this step are normalized to the (0,1) range (see the plot in Figure 7(c)). These curves in Figure 7(c) are exactly the phase fraction-temperature curves that we will use to construct the $\xi - T$ functions.

Table 1. Thermophysical properties of Rubitherm SP 26E

Property	Value	Unit
Melting range	25~27 [23]	[^{o}C]
Freezing range	25~24 [23]	[^{o}C]
L	180	[kJ/kg]
c_p (both phases)	2	[kJ/kg·K]
ρ_{solid}	1.5	[kg/l]
ρliq	1.4	[kg/l]
k (both phases)	~0.5	[W/m·K]

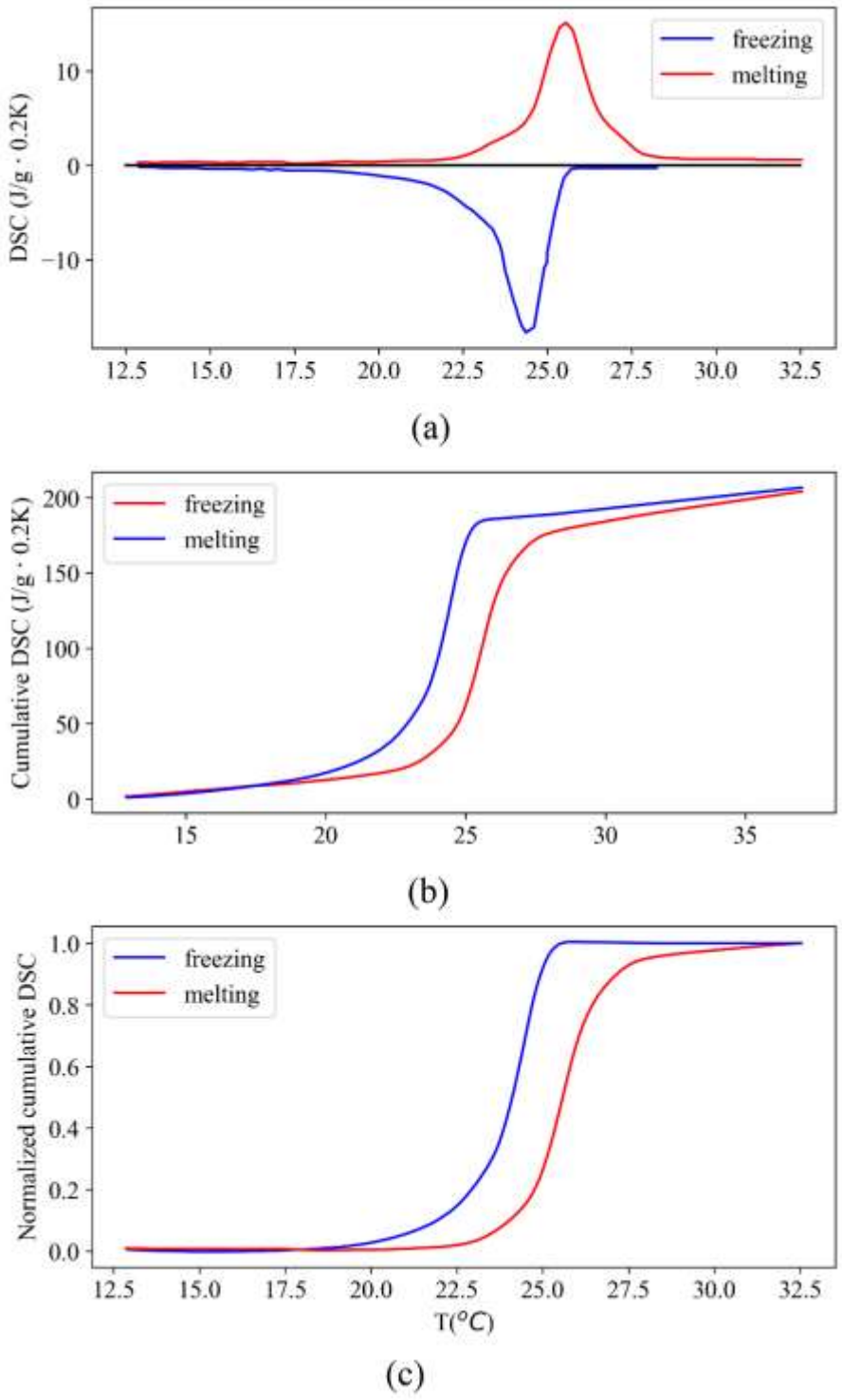

Figure 7**.** DSC data of Rubitherm SP 26E. (a) original measured DSC (b) cumulative DSC (c)cumulative normalized DSC

From the plot in Figure 7(c), the curve parameters for $\xi - T$ curves (Eq. (12) and Eq. (13)) of both freezing and melting processes could be estimated. In this paper, the least square method is employed for the estimation. The least-square estimation method estimates model parameters by minimizing the sum of the square errors (SSE) between calculated and measured values. Eq. (13) is the mathematical representation of the sum of the square errors of our curve models. An optimization problem is formulated and solved to minimize the SSE for both melting and freezing functions.

$$SSE_{err}^2 = \frac{1}{n-1}\sum(\xi_i - \hat{\xi}_i)^2 \tag{13}$$

where ξ_i and $\hat{\xi}_i$ are the measured and the estimated phase fractions, respectively.

Table 2. $\xi - T$ curve parameter estimation results

	Tp (^{o}C)	τ_1	τ_2
Melting	26.0	2.2	0.5
Freezing	24.1	3.0	1.0

Table 2 shows the curve fitting results for both melting and freezing curves. From this table, the peak melting point and freezing point of the PCM are 26.005^{o}C and 24.114^{o}C, respectively, which are consistent with the property data listed in Table 1.The curve fitting results are shown in Figure 8, which clearly shows that the results are in good agreement with an R^2 value between the DSC data and the model higher than 99%.

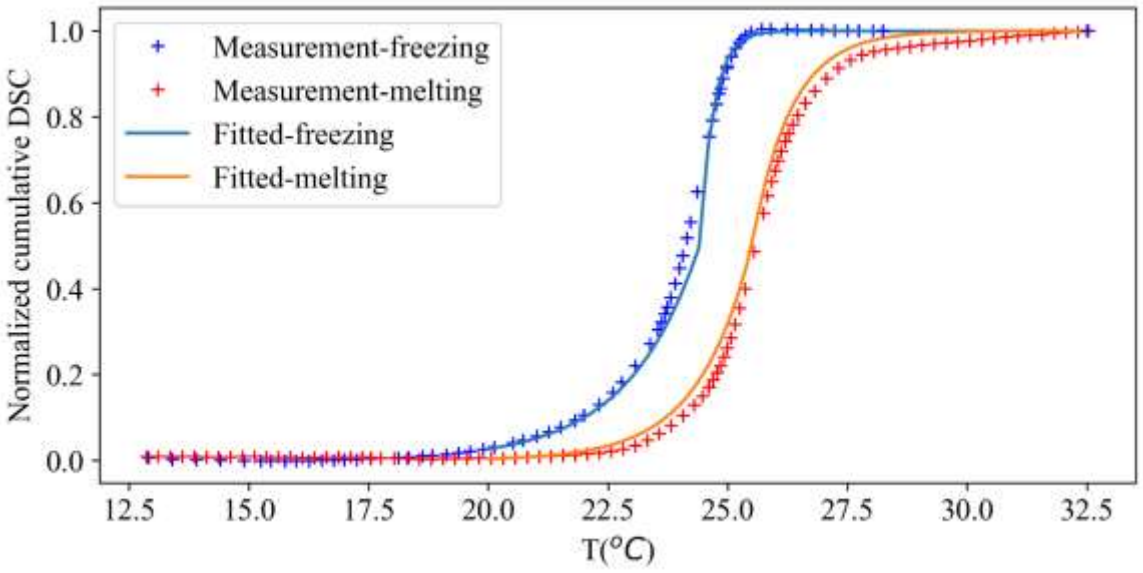

Figure 8**.** Fitting results of $\xi - T$ curves for Rubitherm SP 26E

3.2. Experimental data description

The experimental data are taken from a study by Goia et al. [17], and the experimental setup is briefly introduced here. Figure 9 shows the layout of the measured specimen—the sandwich wall panel, which has two gypsum board layers and a PCM layer in between. Detailed dimensions of the specimen can be found in [8]. Temperatures were measured by thermocouples, with two placed on the upper and lower surfaces and one in the middle of the PCM specimen.

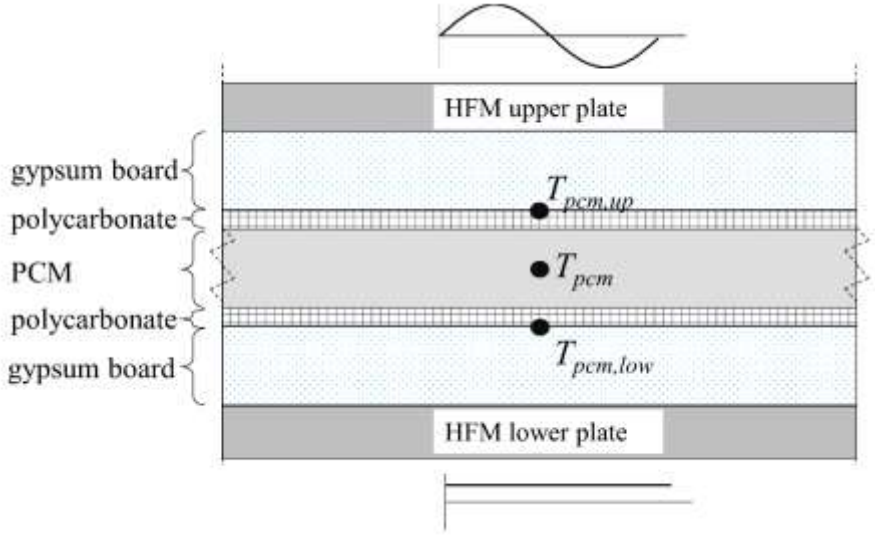

Figure 9**.** The layout of the sandwich wall panel (adapted from [17])

The Heat Flow Meter Apparatus was then used to conduct dynamic experiments. Specifically, a sinusoidal temperature solicitation with a period of 24 h was imposed in the upper place while the lower plate was maintained at 26^{o}C. The test duration of this experiment was two sinusoidal cycles (i.e., 48 hours), while the first few hours were just for an initialization period. In addition, two groups of tests were carried out with different amplitudes for the sinusoidal signals (i.e., ±12^{o}C for the complete phase change scenario and ±6^{o}C for the incomplete phase change scenario).

3.3. Simulation of the PCM panel in EnergyPlus

Based on the heat flux experiments described in section 3.2, two EnergyPlus models using the proposed hysteresis methods were constructed for complete and incomplete phase change cases. To control the temperature profile of the upper and lower plates, methods like the one used in [17] were employed where the surface convection coefficient is set to infinitely high, and the surface outside temperature is given in a schedule. The upper surface of the wall panel (see Figure 9) was forced as the same sinusoidal temperature profiles as that of the experiments. That is, a sinusoidal temperature profile with an average value of 26^{o}C and an amplitude of ±12^{o}C was set

for the complete phase change scenario, and another profile with an amplitude of ±6°C was set for the incomplete phase change scenario. Besides, the periods of both the complete and incomplete sinusoidal temperature wave are one day. For the lower surface of the wall panel, the surface temperature was always kept at 26°C. Then, one phase change hysteresis object was created with the properties given in Table 1 and curve parameters in Table 2.

The EnergyPlus simulation environment is configured with the Conduction Finite Difference method as the heat balance algorithm and 20 timesteps per hour (i.e., a timestep of three minutes). The simulation timestep could be changed to get more accurate results. However, this should be in the range of one to three minutes because three-minute is the longest timestep for the Conduction Finite Difference method, and one minute is the shortest timestep allowed by EnergyPlus.

Three methods of modeling PCM were in the EnergyPlus simulation environment. (1) The proposed two-phase method uses two-phase fraction-temperature curves for both freezing and melting processes (Figure 8); (2) the Current E+ method uses two enthalpy-temperature curves for both freezing and melting processes (Figure 2). This method is also illustrated in Figure 5 as path 1-n-2c; (3) EMS-based method using the EnergyPlus EMS approach presented in this study [17]. This method also uses two enthalpy-temperature curves for both freezing and melting processes (Figure 2). In Figure 5, this method is illustrated as path 1-1´-2d. The properties of the PCM in the simulation are all using that of Rubitherm SP 26E (Table 1).

3.4. Results

The simulation results for all these three different methods are demonstrated in Figure 10 and Figure 11. The temperature presented herein is the node T_{pcm}, the temperature at the center of the PCM layer in Figure 9. To quantitively compare the performance of these three methods, the following indices are used based on [35] and recommended in ASHRAE Guideline 14 [36] to quantify the model accuracy.

- MBE (Mean Bias Error) is calculated according to Eq. (14), which is the average of the errors between simulated results and experimental measurements for node temperature in the middle of the PCM layer, T_{pcm}.

$$MBE = \frac{\sum_{i=1}^{n} |s_i - e_i|}{n} \tag{14}$$

where n is the total number of the observations in a certain experiment, s_i and e_i are the simulated and experimental values, respectively.

- RMSE (Root Mean Square Error) is calculated according to Eq. (15). To avoid cancellation problems, it calculates the squared errors between simulated and experimental values for T_{pcm}.

$$RMSE = \sqrt{\frac{\sum_{i=1}^{n}(s_i - e_i)^2}{n}} \quad (15)$$

• R^2 score is defined as Eq. (16), which is a widely used statistical index to measure how good the simulation model could match with the experimental values. It takes a value between 0.00 and 1.00, where a larger R^2 means a better match between simulated and experimental values for T_{pcm}..

$$R^2 = 1 - \frac{\sum_{i=1}^{n}(s_i - e_i)^2}{\sum_{i=1}^{n}(e_i - \bar{e})^2} \quad (16)$$

In **Table 3.** Error indices for different hysteresis Table 3, the values of these three indices for two scenarios (i.e., complete and incomplete phase change) are presented.

Table 3. Error indices for different hysteresis methods

Scenario	Method	MBE	RMSE	R^2
		[°C]	[°C]	[-]
Complete	Two-phase method	0.50	0.80	0.92
	Current E+ method	0.53	0.83	0.91
	EMS-based method	0.85	1.03	0.89
Incomplete	Two-phase method	0.59	0.80	0.68
	Current E+ method	0.57	0.68	0.44
	EMS-based method	0.55	0.61	0.58

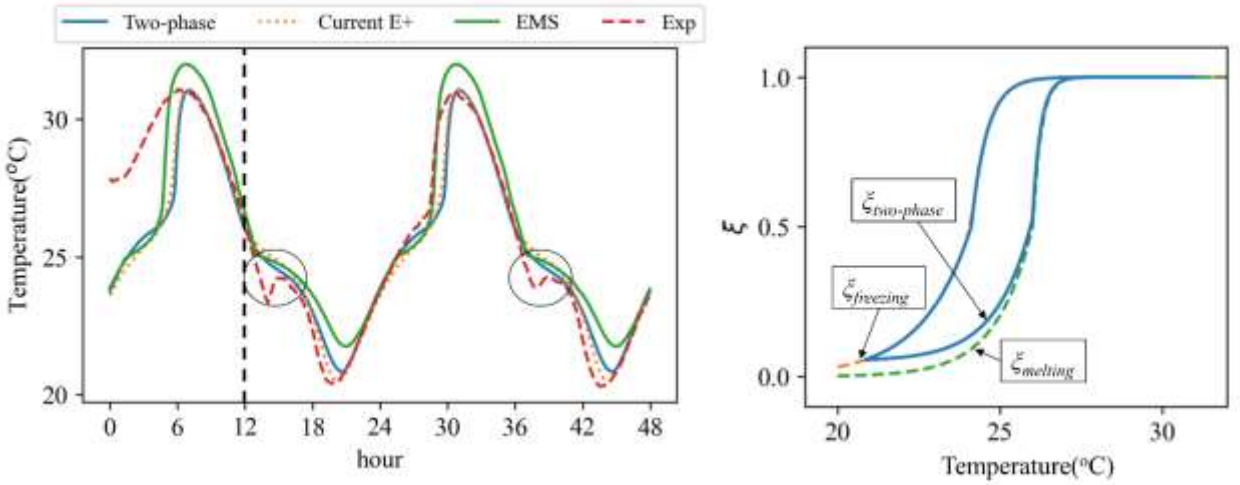

(a) (b)

Figure 10. PCM temperature evolution during the complete phase change process. (a) comparison between experimental data and simulations. (b) corresponding simulation phase fractions for the proposed two-phase method in the $\xi - T$ plane.

Figure 10 shows the PCM temperature profiles for all three methods and experimental values for the complete phase change case. The first few hours of the experiments are initialization periods and are the same for all three cases; the validation starts from the 12th hour. A qualitative inspection of Figure 10(a) shows that the proposed two-phase method and the current EnergyPlus model method show a clearly better match with the experimental values compared to the "EMS" method. This could also be quantitively confirmed from Table 3, where both these two methods resulted in smaller MBE and RMSE values and larger R^2 scores. This suggests that the hysteresis effects are better accounted for by these two methods.

Besides, it could also be observed that the simulated results from both the two-phase method and the current EnergyPlus model are nearly identical. This is because in the complete phase change process where no significant transitional behaviors are recorded, the proposed $\xi - T$ algorithm and the default *H-T* algorithm used in EnergyPlus are interchangeable.

There are, however, significant mismatches between the experimental and simulated temperature values for all three methods for a short period after the start of the cooling period (see the parts circled in Figure *10*(a)). This is because none of the three models considers the supercooling behavior. Consequently, the simulated temperatures after supercooling are higher than the experiment. Following the definition in other studies, supercooling of a PCM in this study means "the delay in the start of freezing process" [37].

The corresponding simulated phase fractions for the proposed two-phase method can be seen in Figure 10(b). It could be observed that the freezing process closely followed the freezing curves while the melting process adopted an intermediate curve close to the melting curve. This slight divergence is because the PCM has not fully crystallized because the endpoint of the freezing process for this PCM is around 18 ^{o}C (see Figure 8).

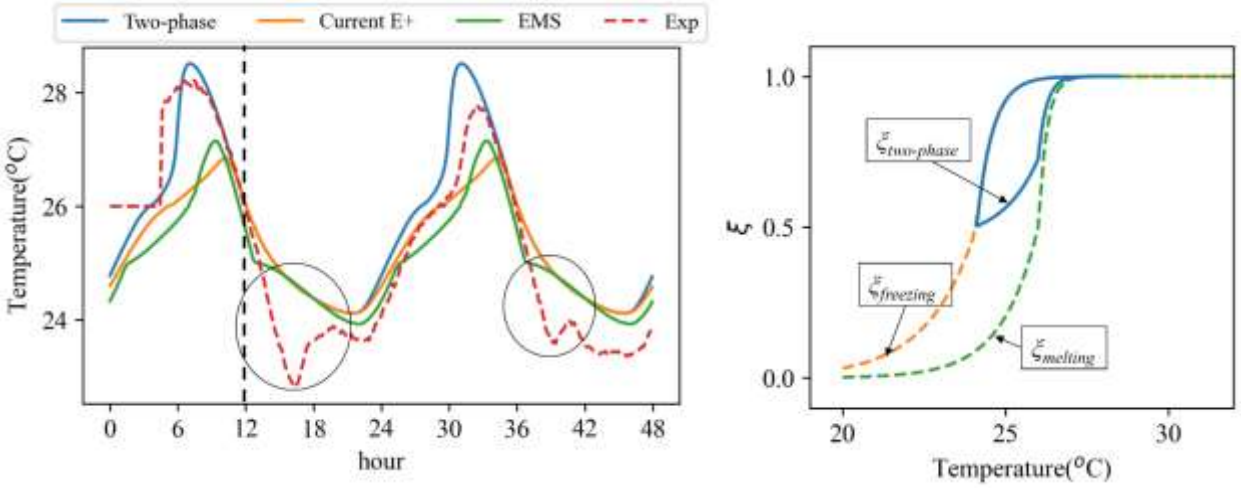

(a) (b)

Figure 11. PCM temperature evolution during incomplete phase change process. (a) comparison between experimental data and simulations. (b) corresponding simulation phase fractions for the proposed two-phase method in the $\xi - T$ plane.

Figure 11 shows the PCM temperature profiles for these three methods and experimental values for the incomplete phase change case. Compared to the complete case, larger errors are observed for all three methods. As shown in the circled parts in Figure 11(a), the mismatch due to the supercooling effect is even more significant in this case. One possible reason is that unlike the temperature profiles shown in Figure 10(a), where the impact of supercooling effect has nearly faded away at the end of the freezing process, the divergence in Figure 11 was still remarkable at the end of the freezing process(i.e., when the hour reached 24). An immediate consequence of this is that the onset point of melting processes at hour 24 in all three simulation methods is approximately one degree Celsius higher than that in the experimental case. As a result, clear mismatches between the simulated results during the following melting process after this onset point and the experimental values are observed (i.e., when the hour is between 24 and 30 in Figure 11). However, Figure 11 highlights that the temperature profile of the proposed two-phase method when the hour is between 24 and 30 has a more similar shape to the experimental results compared with the other two methods. This could be further confirmed with the R^2 score of these three methods because the two-phase method has a significantly higher R^2 score and a higher R^2 score means the simulated results could replicate the experimental results in a better degree.

The effect of supercooling has long been recognized as a problem for the simulations of PCMs[38], and because the freezing process critically depends on the supercooling level, the neglect of supercooling might be problematic in some cases. Supercooling is caused mainly by nucleation and crystal formation mechanisms, and it prevents the freezing process from starting at the nominal temperature. Instead, a temperature drop below the freezing temperature is required to initialize the nucleation of the solid phase. There are a few studies attempting to solve this issue. In the study by Uzan et al. [28], a parameter was used to predict the degree of supercooling that the PCM reaches and determine the enthalpy-temperature relationship of the PCM. The validation results showed that their model corresponded fairly well to their experimental results. However, the model presented is not a macroscopic model method and might be challenging to be applied to PCM-based building components. Also, as pointed out by Barz et al. [24] the supercooling effects are rarely considered in current macroscopic model and further studies are required.

4. Case study of PCM-based building envelope in EnergyPlus

A case study was conducted to investigate the effect of adopting the proposed two-phase method in the whole building energy simulation using EnergyPlus. The simulated building is a single-story one-zone office building in Denver, Colorado, with PCM wallboard on all four external

vertical walls. This case study investigates the impact of different PCM hysteresis algorithms on the simulation of heating/cooling load, and the zone mean air temperature. The simulated zone uses an ideal load air system where the cooling/heating rates of this system are exactly the cooling/heating load of the conditioned zone. Three sets of simulations were carried out using the same building model with different PCM hysteresis algorithms: (1) the proposed two-phase method; (2) the current E+ PCM method with default hysteresis model; (3) without hysteresis where the current single-curve PCM method in EnergyPlus was used without considering hysteresis effects. The properties of Rubitherm SP 26E (Table 1) are used for all three cases, while only one enthalpy-temperature curve is used, and this curve is obtained as the average of the freezing and melting curves shown in Figure 2.

First, three simulations were carried out to study the cooling/heating rate in different weather conditions when a partial phase change could be observed. The hourly heating/cooling rate comparisons are shown in Figure 12. The heating/cooling rates were found to be the same with the two-phase method and current E+ method before the "valley" (or "peak" for the cooling case), and then significant differences could be observed after that. This is consistent with the results presented in Section 3.4. That is, the proposed two-phase method yielded the same results as the current E+ method before the phase change process was interrupted. After the interruption, as long as partial phase transitions occurred, the results with the two-phase method showed a significant difference from the results with the current E+ method. In this case, the maximum difference between these two methods was close to 20%. Also, the heating/cooling rates with the proposed two-phase method were found to be different even before the "valley" (or "peak" for the cooling case) when compared to the non-hysteresis method. This is because the results of the non-hysteresis method started to diverge after the phase change process began.

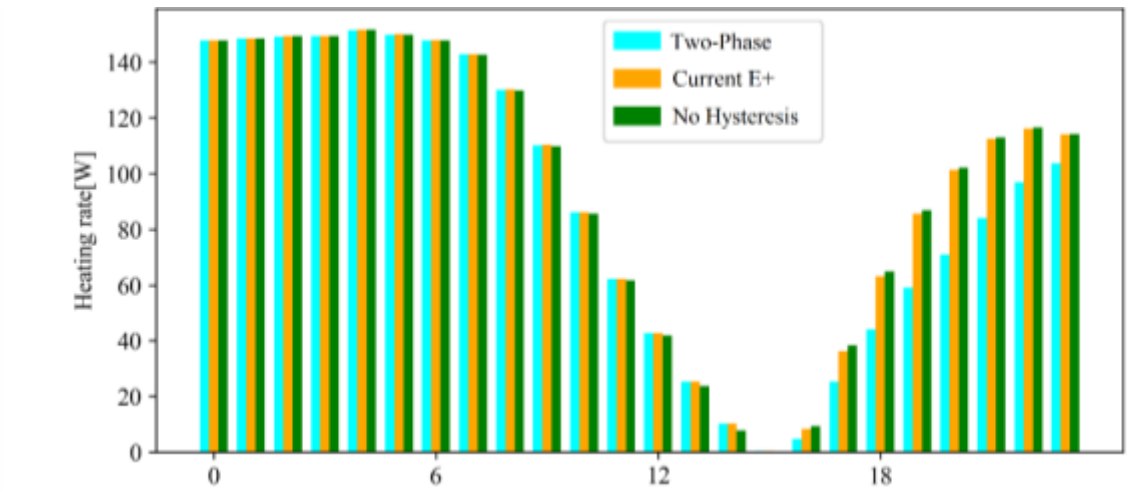

(a)

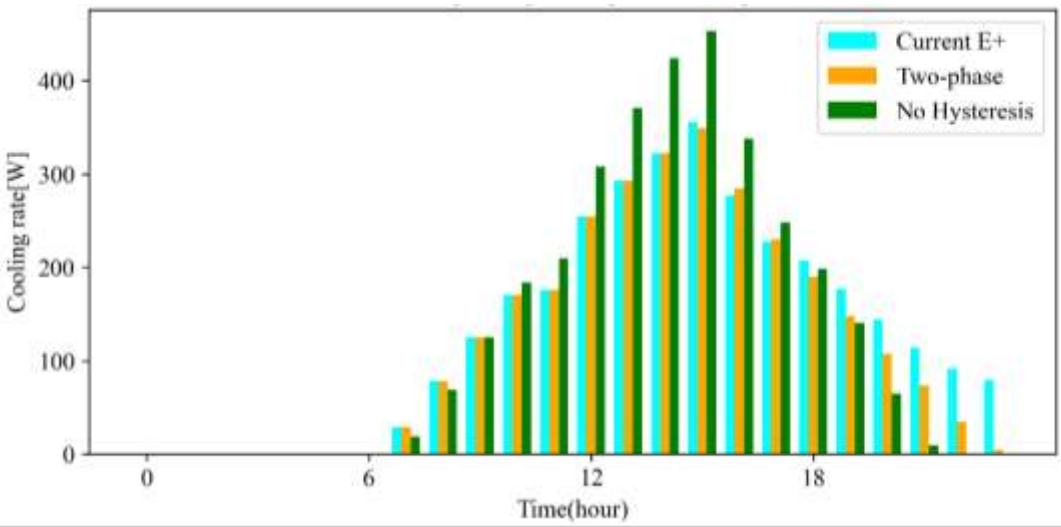

(b)

Figure 12. (a) hourly heating loads comparison (b) hourly cooling load comparison

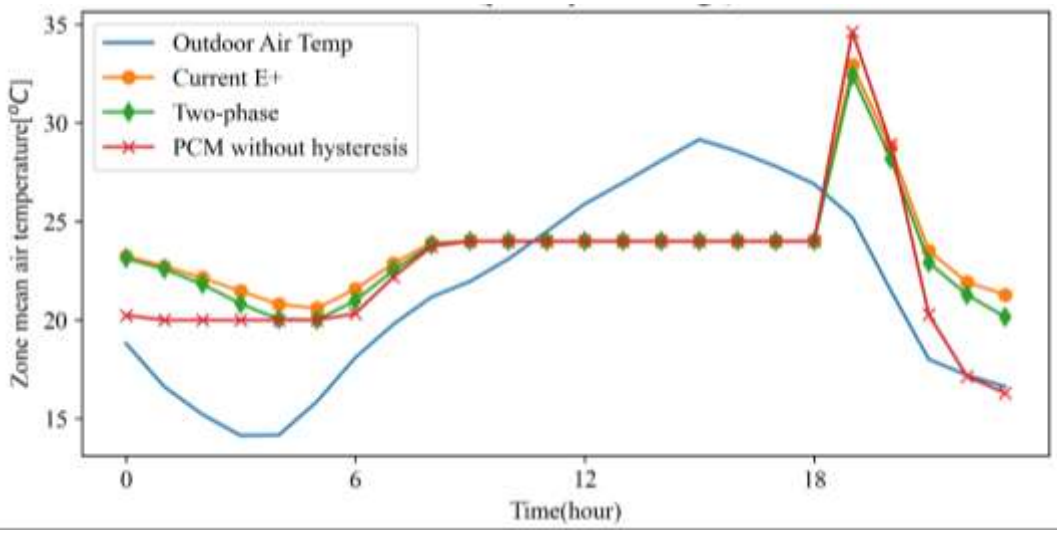

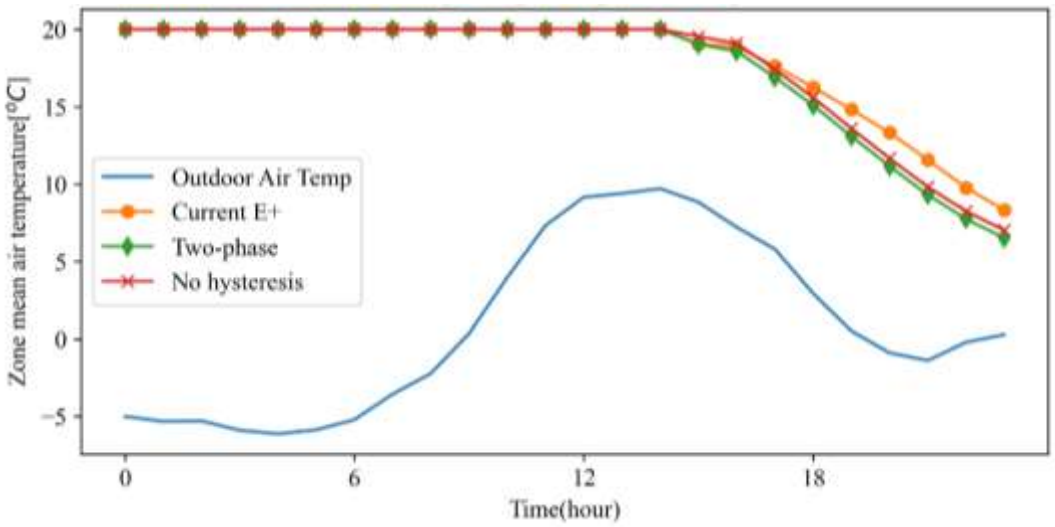

Figure 13. Hourly zone mean air temperature comparison (a) for cooling case; (b) for heating case

Then, another set of simulations were carried out to study the effects of the PCM hysteresis methods on the thermal storage capacity of the PCM building envelope or the operation schemes when PCM is used as a demand response source (e.g., load shifting). These three simulations are based on the same building models with different operation schedules. For the cooling season, the cooling system was staged off after 18:00, and for the heating season, the heating system was turned off after 14:00. These on-off operation schedules are intentionally designed to make sure the PCM could experience partial phase change processes. From Figure 13, the maximum differences in zone mean air temperature between the two-phase method and the current E+ method in both heating and cooling cases were approximately 1^{o}C. Therefore, if the PCM-based envelope is used as a demand response source by shifting the heating/cooling from peak period to off-peak period while still maintaining the same thermal comfort, the optimal operation schemes in these two methods will certainly be different if partial phase transitions are involved.

Last, three other simulations were carried out to study the cooling/heating rate in design conditions, which were also meant to compare the HVAC equipment sizing results using different PCM hysteresis algorithms. The results are shown in Figure 15. The difference in cooling rate between the two-phase method and the current E+ method is small. As PCM temperature profiles in Figure 15 (c) and Figure 15 (d) illustrate, no partial phase transition was recorded in both cases. Section 3.4 explains that for complete phase change processes, the proposed two-phase methods will output similar results as the current E+ method. Besides, the cooling rates in the hysteresis models, both the two-phase method and the current E+ method, showed a clear decrease when compared to the non-hysteresis model. This is because the hysteresis effect is quite significant to the PCM layer temperature, as shown in Figure 15 (c). In the heating case, both the heating rate and PCM layer temperature are nearly the same in all these three methods, as shown in Figure 15 (d). This is because no phase change was recorded, as

could be seen in Figure 15 (d), that the phase change temperatures of the materials are higher than the temperature of the PCM layer in the heating case. Therefore, the proposed hysteresis model does not show clear advantages in design conditions compared to the current E+ method. Hence, the equipment sizing results will also be similar between the proposed model and the current E+ model.

In addition, from Figure *14* we can observe the composition between complete phase change and partial phase change in one week from July 1st to July 7th in the cooling case. It can be observed that in the early morning of the first two days and the last day of this week, the PCM layer started to freeze as the outdoor air temperature dropped, while before the freezing cycle was completed at around 6am the PCM layer temperature started to rebound. Besides, there were seven complete phase transitions, either freezing or melting, in this week, as marked in this figure. Therefore, partial phase change occurred quite frequently in this week, which means that it is necessary to apply a better PCM model to account for the hysteresis effects. It should be noted that the frequency of occurrences of phase transition depends on the weather conditions, the PCMs' thermal properties, etc. Therefore, the PCMs in building applications should be properly selected and designed to improve the frequency of occurrences of phase transition to better leverage its latent thermal capacities.

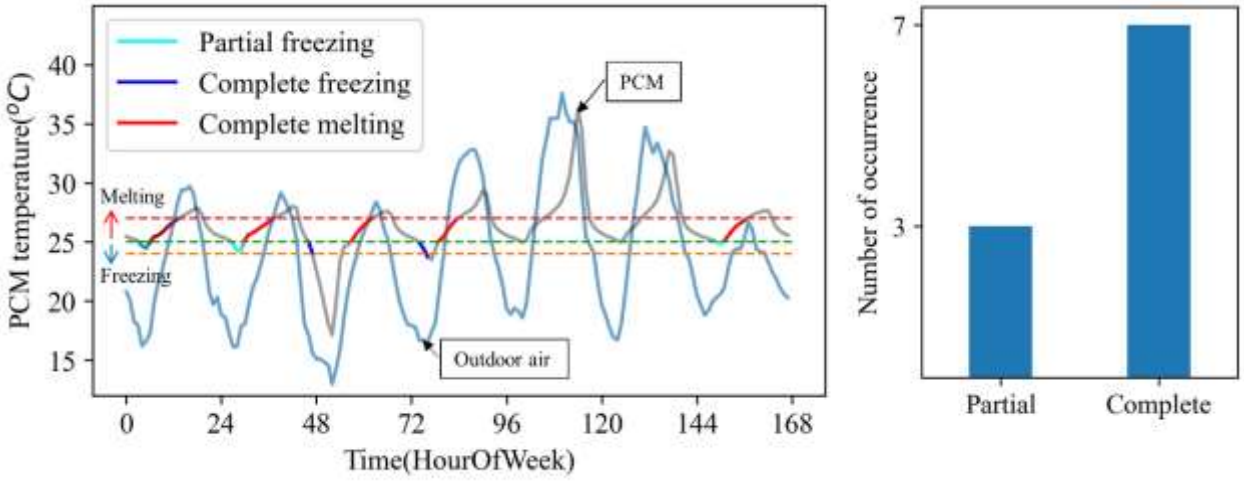

Figure 14. (a) PCM layer temperature; (b) Number of occurrences of both partial and complete phase transition

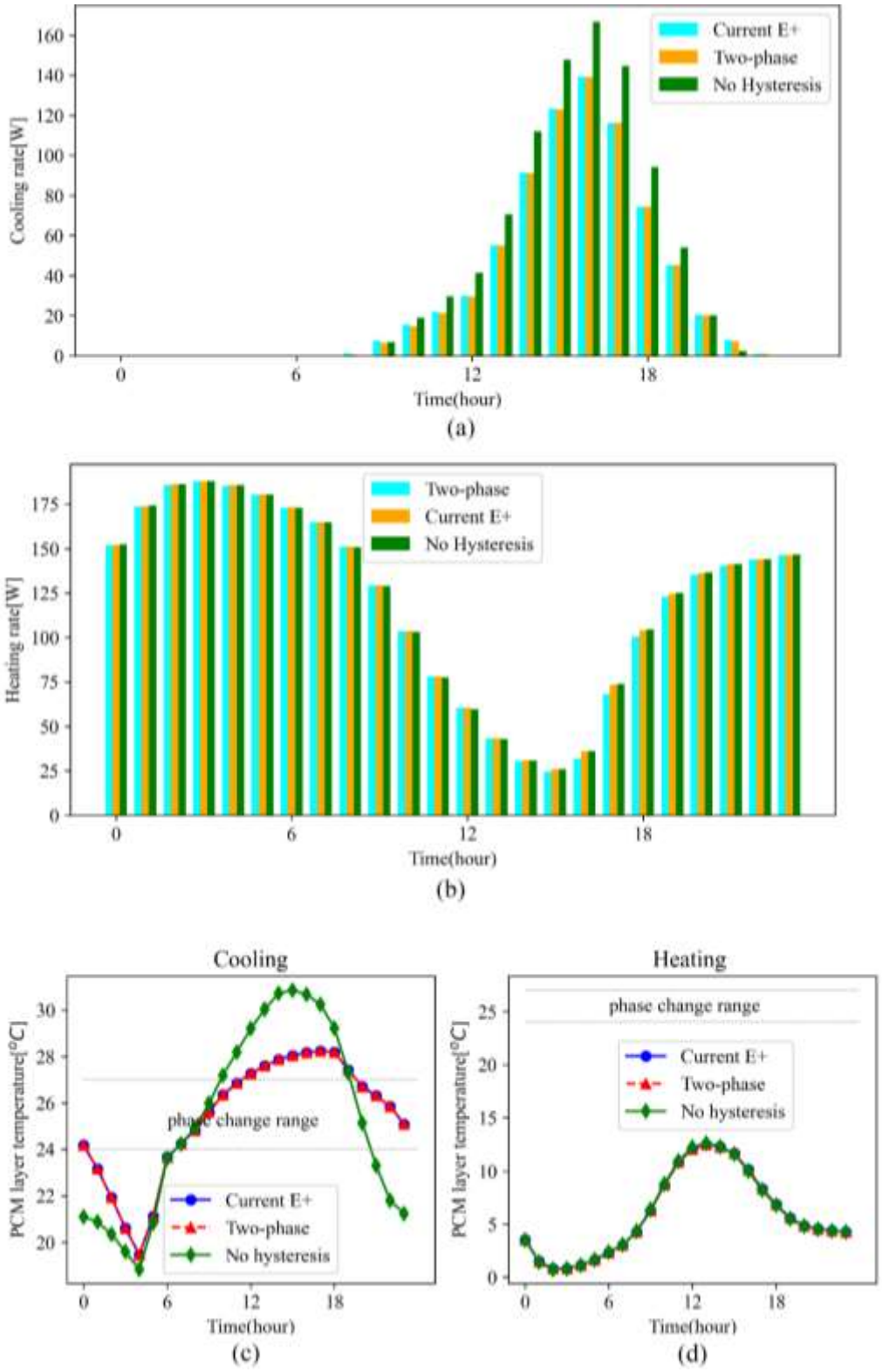

Figure 15. (a) Hourly cooling rate comparison in cooling design conditions (b) Hourly heating rate comparison in heating design conditions (c) PCM layer temperature comparison in cooling design conditions (d) PCM layer temperature comparison in heating design conditions

5. Parameter sensitivity analysis

Validation results in Section 3 suggest that the proposed two-phase model could provide accurate results compared to experimental data. At the same time, it is still not completely accurate when was applied to the partial phase change process. Within the simulation model using the proposed two-phase method in Section 3.3, in addition to the $\xi - T$ curve parameters, many other parameters may also influence the model accuracy and are often specified by the manufacturers' data sheets which might be inaccurate due to various reasons (e.g., measurement uncertainties, improper storage, etc.). In this section, taking the simulation model in section 3 for an incomplete phase change scenario that uses the proposed hysteresis method as an example, a sensitivity analysis was performed to identify the parameters that have significant influences on the final errors between the simulation results and experiment results. These results could serve as a guideline for the priority of accurate measurement of PCM thermophysical properties.

5.1. Sensitivity analysis methodology

The sensitivity analysis includes 13 parameters that represent the thermo-physical properties of the PCM. Table 4 shows these parameters as well as their probability distributions. The property parameters (e.g., density) were assumed to be normally distributed, and a perturbation of 5% was used as their variances based on the spec sheet of Rubitherm SP 26E. For the curve parameters of both freezing and melting process (e.g., $T_{p,metling}$), they were assumed to follow a uniform distribution and a perturbation of ±5% were also applied to their nominal values. The output of the sensitivity analysis is the R^2 value between the simulation and experimental results for the node temperature in the middle of the PCM layer, T_{pcm}.

Table 4. Probability distributions of the parameters studied

Parameter	Distribution	Unit	Source
Thermal Conductivity(*solid*), k_{solid}	N (0.5,0.025^2)	[W/m·K]	[23]
Density(*solid*), ρ_{solid}	N (1.5,0.075^2)	[kg/l]	[23]
Specific heat capacity(*solid*), $c_{p,solid}$	N (2,0.1^2)	[kJ/kg·K]	[23]
Thermal Conductivity(*liquid*), k_{liq}	N (0.5,0.025^2)	[W/m·K]	[23]
Density(*liquid*), ρ_{liq}	N (1.4,0.07^2)	[kg/l]	[23]
Specific heat capacity(*liquid*), $c_{p,liq}$	N (2,0.1^2)	[kJ/kg·K]	[23]
Latent Heat (LH)	N (180,9^2)	[kJ/kg]	[23]
$T_{p,m}$	U (21.70,26.53)	[^{o}C]	N/A
$\tau_{1,m}$	U (0.87,1.07)	[^{o}C]	N/A
$\tau_{2,m}$	U (2.69,3.29)	[^{o}C]	N/A
$T_{p,f}$	U (23.40,28.61)	[^{o}C]	N/A
$\tau_{1,f}$	U (0.45,0.55)	[^{o}C]	N/A
$\tau_{2,f}$	U (2.01,2.45)	[^{o}C]	N/A

The sensitivity analysis approach used in this study is a variance-based method, namely, the Sobol method. Sobol method is viewed as one of the most efficient sensitivity analysis [39], and there exist many successful applications in the building field [40-42]. Sobol is a form of a global sensitivity analysis, and it could decompose the variance of the output into the uncertainties of inputs or sets of inputs. More detail on Sobol can be found in [39]. Besides, a python package of sensitivity analysis methods which provides an easy-to-use implementation of Sobol was used to help conduct the proposed sensitivity analysis [43].

5.2. Sensitivity analysis results

Figure 16 shows the sensitivity coefficient for all 13 parameters in descending order of importance. It could be observed that the most influential parameters are the curve parameters of both freezing and melting processes and the latent heat capacity. This further highlights the phase change processes of the materials must be carefully measured, and on-site DSC testing might be required to validate the manufacturers' catalog data. Besides, these results also justify the need to have a hysteresis model.

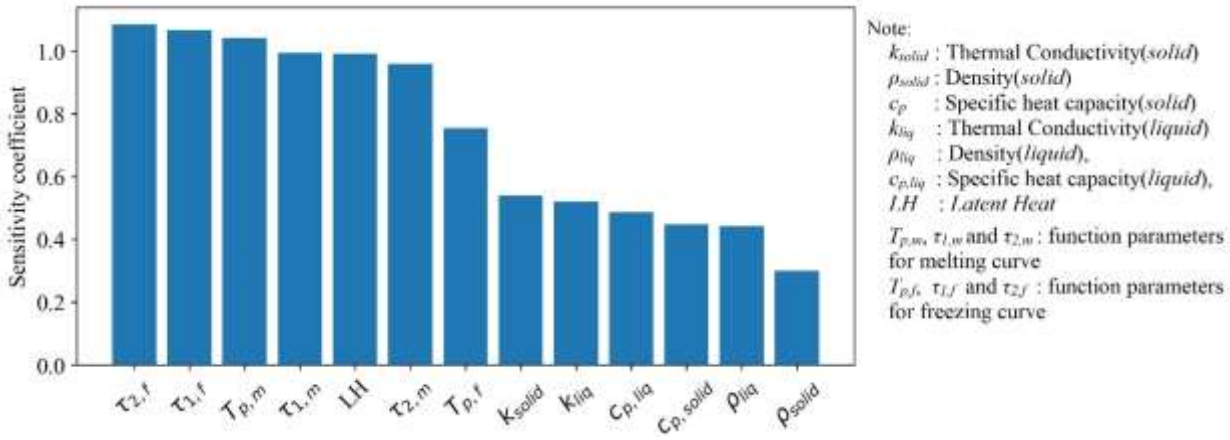

Figure 16. Sensitivity coefficient of the selected 13 parameters

6. Conclusion and future work

6.1. Summary and conclusion

This paper proposed a modeling method for PCM-based building components based on a "two-phase" assumption and is aimed to model the hysteresis effect of PCMs with improved accuracy compared with currently available models, especially during the incomplete phase transition process. While the proposed model was implemented and investigated in EnergyPlus, it can also be easily implemented in other building simulation programs such as Modelica and TRNSYS.

This method was tested for both complete and partial phase transition processes and compared with several existing approaches. Comparisons between experimental and simulation results show:

1) For the complete phase change scenario, both the proposed method and the current hysteresis method in EnergyPlus could achieve a good agreement with experimental data. However, the experimental results clearly show supercooling effects exist during the freezing process, and all these methods are unable to model the supercooling behaviors.
2) For the partial phase change scenario, the proposed method could lead to significant improvements compared to other alternative methods, while disagreements still could be observed in the partial phase transition. These results indicate that supercooling has a more significant impact on the partial phase transition.

Annual building simulations using EnergyPlus were performed to study the performance of this two-phase PCM hysteresis model regarding heating/cooling rates and zone mean air temperature. The results showed that significant changes were observed in both heating/cooling loads and zone mean air temperature when partial phase transitions were recorded.

6.2. Limitations and future work

From the comparison results, an important observation is that supercooling effect should be accounted for to improve the accuracy of PCM modeling methods. Up to date, there are already a few promising modeling methods for supercooling behaviors of PCMs. For example, in 2021, Thonon et al. proposed a method to model the supercooling process of PCMs [44] analytically. In their method, modeling supercooling is achieved by dividing the supercooling process into three steps: metastable state, recalescence, and regular solidification. However, further studies are required to develop the most computationally efficient and reliable modeling method for supercooling in building simulation programs.

The observation from the sensitivity analysis is that the $\xi - T$ curves or the enthalpy-temperature curves, which are used to characterize the phase transition processes, are of great importance to the accuracy of simulation results. However, there are still many issues that prevent us from getting accurate and reliable data. For example, the enthalpy-temperature curve of a PCM is usually measured using a DSC analysis on small quantities of the materials under conditions that might be different from the operating conditions in real build structures. Besides, improper storage may also make the PCM properties inconsistent with the catalog data from manufacturers. Another issue that has been widely perceived is that DSC analyses alone are not sufficient to provide input data for simulation tools. Therefore, further studies are required to improve the characterization of the PCM's thermophysical properties.

Besides, the hysteresis model proposed in this study is only a static method which means the phase fraction of the PCMs only depends on the temperature or the direction of the temperature change. However, it has been known for many years that the cooling/heating rate of the PCMs would also influence the resulting phase fraction-temperature curves. Therefore, dynamic hysteresis models, also called rate-dependent hysteresis models, are required to account for these

dynamic behaviors. In the future, studies are still required to model this dynamic behavior of PCMs in building simulation programs if further improvements to simulation models are required.

7. Acknowledgement and Disclaimer

The research reported in this paper was partially supported by the Building Technologies Office at the U.S. Department of Energy through the Emerging Technologies program under award number DE-EE0008677.

Reference

[1] A. de Gracia, Dynamic building envelope with PCM for cooling purposes–Proof of concept, Applied energy, 235 (2019) 1245-1253.
[2] P.K.S. Rathore, S.K. Shukla, An experimental evaluation of thermal behavior of the building envelope using macroencapsulated PCM for energy savings, Renewable Energy, 149 (2020) 1300-1313.
[3] R. Ansuini, R. Larghetti, A. Giretti, M. Lemma, Radiant floors integrated with PCM for indoor temperature control, Energy and Buildings, 43 (11) (2011) 3019-3026.
[4] H. Akeiber, P. Nejat, M.Z.A. Majid, M.A. Wahid, F. Jomehzadeh, I.Z. Famileh, J.K. Calautit, B.R. Hughes, S.A. Zaki, A review on phase change material (PCM) for sustainable passive cooling in building envelopes, Renewable and Sustainable Energy Reviews, 60 (2016) 1470-1497.
[5] M. Pomianowski, P. Heiselberg, Y. Zhang, Review of thermal energy storage technologies based on PCM application in buildings, Energy and Buildings, 67 (2013) 56-69.
[6] F. Souayfane, F. Fardoun, P.-H. Biwole, Phase change materials (PCM) for cooling applications in buildings: A review, Energy and buildings, 129 (2016) 396-431.
[7] P. Moreno, A. Castell, C. Sole, G. Zsembinszki, L.F. Cabeza, PCM thermal energy storage tanks in heat pump system for space cooling, Energy and buildings, 82 (2014) 399-405.
[8] S. Fantucci, F. Goia, M. Perino, V. Serra, Sinusoidal response measurement procedure for the thermal performance assessment of PCM by means of dynamic heat flow meter apparatus, Energy and Buildings, 183 (2019) 297-310.
[9] A. Kylili, P.A. Fokaides, Numerical simulation of phase change materials for building applications: a review, Advances in Building Energy Research, 11 (1) (2017) 1-25.
[10] T. Barz, A. Sommer, Modeling hysteresis in the phase transition of industrial-grade solid/liquid PCM for thermal energy storages, International Journal of Heat and Mass Transfer, 127 (2018) 701-713.
[11] P.C. Tabares-Velasco, C. Christensen, M.J.B. Bianchi, Environment, Verification and validation of EnergyPlus phase change material model for opaque wall assemblies, 54 (2012) 186-196.
[12] N. Brown, S. Philip, I.S. Trojaola, S. Ubbelohde, G. Loisos, Calibration of an Energyplus Simulation of a Phase Change Material Product Using Experimental Test Cell Data, in: Building Simulation Conference, 2014, pp. 268-275.
[13] P. Dolado, A. Lazaro, J.M. Marin, B. Zalba, Characterization of melting and solidification in a real-scale PCM–air heat exchanger: Experimental results and empirical model, Renewable Energy, 36 (11) (2011) 2906-2917.
[14] P.W. Egolf, H. Manz, Theory and modeling of phase change materials with and without mushy regions, International Journal of Heat and Mass Transfer, 37 (18) (1994) 2917-2924.
[15] B. Delcroix, M. Kummert, A. Daoud, Development and numerical validation of a new model for walls with phase change materials implemented in TRNSYS, Journal of Building Performance Simulation, 10 (4) (2017) 422-437.

[16] J. Bony, S. Citherlet, Numerical model and experimental validation of heat storage with phase change materials, Energy and Buildings, 39 (10) (2007) 1065-1072.
[17] F. Goia, G. Chaudhary, S. Fantucci, Modelling and experimental validation of an algorithm for simulation of hysteresis effects in phase change materials for building components, Energy and Buildings, 174 (2018) 54-67.
[18] R. Chandrasekharan, E.S. Lee, D.E. Fisher, P.S. Deokar, An Enhanced Simulation Model for Building Envelopes with Phase Change Materials, ASHRAE Transactions, 119 (2) (2013).
[19] Y. Ivshin, T.J. Pence, A constitutive model for hysteretic phase transition behavior, International Journal of Engineering Science, 32 (4) (1994) 681-704.
[20] S. Al-Saadi, Z. Zhai, TRNSYS Type 285-Phase Change Materials Embedded in Wall System, Boulder, CO, (2014).
[21] A. Halimov, M. Lauster, D. Müller, Validation and integration of a latent heat storage model into building envelopes of a high-order building model for Modelica library AixLib, Energy and Buildings, 202 (2019) 109336.
[22] A. Fallahi, N. Shukla, J. Kosny, Numerical thermal performance analysis of PCMs integrated with residential attics, Proceedings of SimBuild, 5 (1) (2012) 431-439.
[23] Rubitherm, https://www.rubitherm.eu/media/products/datasheets/Techdata_-SP26E_EN_09112020.PDF, (2020).
[24] T. Barz, A.J.I.J.o.H. Sommer, M. Transfer, Modeling hysteresis in the phase transition of industrial-grade solid/liquid PCM for thermal energy storages, 127 (2018) 701-713.
[25] D.B. Crawley, L.K. Lawrie, F.C. Winkelmann, W.F. Buhl, Y.J. Huang, C.O. Pedersen, R.K. Strand, R.J. Liesen, D.E. Fisher, M.J. Witte, EnergyPlus: creating a new-generation building energy simulation program, Energy and buildings, 33 (4) (2001) 319-331.
[26] C.O. Pedersen, Advanced zone simulation in EnergyPlus: incorporation of variable properties and phase change material (PCM) capability, in: Proceedings of building simulation, 2007, pp. 1341-1345.
[27] P.C. Tabares-Velasco, C. Christensen, M. Bianchi, Verification and validation of EnergyPlus phase change material model for opaque wall assemblies, Building and Environment, 54 (2012) 186-196.
[28] A.Y. Uzan, Y. Kozak, Y. Korin, I. Harary, H. Mehling, G. Ziskind, A novel multi-dimensional model for solidification process with supercooling, International Journal of Heat and Mass Transfer, 106 (2017) 91-102.
[29] U. Gaur, B.J.J.o.P. Wunderlich, C.R. Data, Heat capacity and other thermodynamic properties of linear macromolecules. II. Polyethylene, 10 (1) (1981) 119-152.
[30] E.D. Team, EnergyPlus Version 9.6 Engineering Reference: The Reference to EnergyPlus Calculations, EnergyPlus Development Team, US Department of Energy: Washington, DC, USA, (2019).
[31] R.D. Fraser, E. Suzuki, Resolution of overlapping bands. Functions for simulating band shapes, Analytical chemistry, 41 (1) (1969) 37-39.
[32] V.B. Di Marco, G.G. Bombi, Mathematical functions for the representation of chromatographic peaks, Journal of Chromatography A, 931 (1-2) (2001) 1-30.
[33] U.S.A. DOE, New Features in EnergyPlus version 2.0.0, in.
[34] https://github.com/BE-HVACR/Energyplus-EnhancedPCM.
[35] G.R. Ruiz, C.F. Bandera, Validation of calibrated energy models: Common errors, Energies, 10 (10) (2017) 1587.
[36] A. Guideline, Guideline 14-2014: Measurement of Energy Demand and Water Savings, ASHRAE Standards Committee: Atlanta, GA, USA, (2014).
[37] B. Zalba, J.M. Marın, L.F. Cabeza, H. Mehling, Review on thermal energy storage with phase change: materials, heat transfer analysis and applications, Applied thermal engineering, 23 (3) (2003) 251-283.
[38] E. Günther, H. Mehling, S. Hiebler, Modeling of subcooling and solidification of phase change materials, Modelling and Simulation in Materials Science and Engineering, 15 (8) (2007) 879.

[39] A. Saltelli, M. Ratto, T. Andres, F. Campolongo, J. Cariboni, D. Gatelli, M. Saisana, S. Tarantola, Global sensitivity analysis: the primer, John Wiley & Sons, 2008.
[40] V. Zeferina, Sensitivity analysis of cooling demand applied to a large office building, Energy and Buildings, 235 (2021) 110703.
[41] B. Eisenhower, Z. O'Neill, V.A. Fonoberov, I. Mezić, Uncertainty and sensitivity decomposition of building energy models, Journal of Building Performance Simulation, 5 (3) (2012) 171-184.
[42] Z. Pang, Z. O'Neill, Y. Li, F. Niu, The role of sensitivity analysis in the building performance analysis: A critical review, Energy and Buildings, 209 (2020) 109659.
[43] J. Herman, W. Usher, SALib: an open-source Python library for sensitivity analysis, Journal of Open Source Software, 2 (9) (2017) 97.
[44] M. Thonon, G. Fraisse, L. Zalewski, M. Pailha, Analytical modelling of PCM supercooling including recalescence for complete and partial heating/cooling cycles, Applied Thermal Engineering, 190 (2021) 116751.